3MRA: Multi-Criteria Resource Assignment in Multiband Elastic Optical Networks

Tianxiang Li,* Shrinivas Petale,* Gustavo Bittencourt Figueiredo,† and Suresh Subramaniam*
*Department of Electrical and Computer Engineering, George Washington University, Washington, D.C.
†Universidade Federal da Bahia, Salvador, Bahia, Brazil
Email: {tianxiangli, srpetale, suresh}@gwu.edu, gustavobf@ufba.br

***Abstract*—The increasing demand for internet connectivity, driven by advancements in 6G, IoT, and smart home technologies, has intensified the need for expanding network capacity. Although multi-band fiber technology offering substantial capacity gains without requiring immediate fiber replacement has emerged recently, it introduces challenges such as Interband Stimulated Raman Scattering (ISRS), a nonlinear effect causing energy loss, that affects the Quality of Transmission (QoT). This paper presents a novel resource allocation scheme called 3-Metrics Resource Assignment (3MRA) that considers the QoT and spectrum fragmentation. Simulation results show that 3MRA reduces the fragmentation of network resources and lowers the bandwidth blocking probability, and is very helpful in improving network capacity, highlighting its practical value.**

I. Introduction

In the current technological landscape, driven by rapid advancements in 6G, Internet of Things (IoT), and smart home innovations, the demand for internet connectivity is escalating at an unprecedented rate. Consequently, there has been a continuous effort to identify and develop technologies that can expand the carrying capacity of networks. Optical fiber communication, which plays a pivotal role in the core network infrastructure, has been the focus of extensive research. Emerging technologies such as Elastic Optical Networks (EONs), and Space Division Multiplexing (SDM) [1] [2] have been developed to enhance the transmission capabilities of optical fibers.

Recently, with advancements in Erbium-Doped Fiber Amplifiers (EDFAs) for optical signal amplification across different wavelengths, multiband (MB) technology has gained significant attention. In addition, the possibility of using not only C and L bands but also other available bands such as E, O, and S bands has been considered in recent years [3]. Meanwhile some papers focus on the combination of MB and SDM [4] to provide a detailed network upgrade plan [5]. These upgrade strategies can, indeed, effectively enlarge network capacity. However, they also require significant budget due to the necessary upgrades of optical fibers, transceivers, and other equipment, leading to relatively high costs [6]. Therefore, MB itself, which does not require large-scale hardware modifications, offers a cost-saving alternative. This makes it a preferred choice for many operators as the first step in network upgrades.

In the MB scenario, Physical Layer Impairments (PLIs) between adjacent optical signal bands pose challenges [7], as different signals transmitted through the same optical fiber can interfere with each other, leading to signal degradation and unacceptable Quality of Transmission (QoT). Increasing power to boost the Signal-to-Noise Ratio (SNR) exacerbates PLIs, creating a detrimental cycle. To effectively manage resources in such networks, Routing, Modulation, Band, and Spectrum Assignment (RMBSA) plays a critical role in optimizing the allocation of network resources while mitigating interference. Consequently, providing efficient solutions to the RMBSA problem is crucial [8].

Due to the importance of RMBSA with PLIs considered, there is intense research activity in the field, and several resource allocation strategies exist based on considering the MB network environment and calculating QoT [9], and reducing PLIs by placing specific equipment [10]. Previous work [11] has provided models for calculating non-linear interference (NLI) accurately. However, if maintaining a high average SNR across the network is prioritized during the allocation of new connections, the system will tend to assign a new connection to a spectrum region that is far away from that of existing connections. This approach minimizes the SNR degradation of existing connections caused by the new connection and also maximizes the SNR of the new connection itself. The problem with this approach is that it could cause the remaining available spectrum resources to become fragmented. Since network connections require contiguous spectrum resources, fragmented spectrum may prevent high-bandwidth connections from finding available spectrum, even when the total amount of remaining spectrum is sufficient, thereby causing increased network blocking rates. The spectral gap between two connection requests is not the only factor contributing to fragmentation. Another equally important factor is the departure time of connection requests. When two adjacent connection requests have significantly different departure times, even if the first request releases spectrum that can be reused, some other available spectrum could still remain unusable due to the later departure time of the second request, preventing the formation of a contiguous block of available spectrum. Conversely, if two adjacent connection requests have similar departure times, they can release a larger contiguous spectrum block at almost the same time. Therefore, both the spectrum allocated to connection requests and their expected departure times jointly influence the fragmentation they may cause in the network.

When the majority of connection requests have relatively low bandwidth requirements, fragmentation may not cause severe issues, as each request requires only a small amount of spectrum. However, as the data rate of connection requests increases, the spectrum required for each request also grows. Furthermore, when considering the SNR receiver detection threshold in a MB environment, fragmentation becomes an

978-3-903176-67-6

even more critical factor. This is because a single connection request using a lower-order modulation format requires a lower SNR threshold but a larger spectral width. In such cases, fragmentation caused by improper spectrum assignment can cause a large amount of spectrum to be unavailable for requests, causing wastage of precious network resources and a decrease in network capacity [12]. From the foregoing, it is clear that a sophisticated RMBSA algorithm must not only consider the QoT of the arriving and existing connections, but also the fragmentation caused by the resource allocation.

In this paper, we present an innovative 3-Metrics Resource Assignment scheme designed to address these challenges, named 3MRA. Our scheme considers SNR, spectrum position, and connection departure times to make a judicious allocation of resources to an arriving connection request. Simulation results demonstrate that our method improves resource allocation efficiency and reduces blocking probability compared to state-of-the-art approaches, while also significantly reducing the algorithm's execution time, highlighting its substantial practical value and effectiveness.

The rest of this paper is organized as follows. The network model and problem statement are introduced in Section II. The proposed 3MRA algorithm is presented in Section III. Simulation results are presented in Section IV, and the work is concluded in Section V.

II. Network Model, Problem Statement, and Motivation

We consider an EON network with a spectrum slice granularity of 12.5 GHz and two unidirectional single-core optical fibers used for transmission between each pair of physical nodes. The considered wavelength range of the C+L band varies from 1530 nm to 1625 nm. 916 frequency slots (FSs) are available on each fiber, where the C band occupies 399 FSs and the L band occupies 517 FSs [8]. Spectrum assignment respects spectral continuity and contiguity constraints during transmission. We assume that the spectrum allocated to a single request must reside entirely within either the C band or the L band, and cannot be split across both bands. There is 1 FS of guard band between any two adjacent requests. Five different modulation formats (MFs) are considered, namely, BPSK, QPSK, 8-QAM, 16-QAM, and 32-QAM. These MFs are also numbered MF 1 through MF 5, respectively. The number of FSs for various data rates and MFs are given in Table I. The SNR thresholds (SNR_{th}) for MF 1 through 5 are 9 dB, 12 dB, 16 dB, 18.6 dB, and 21.6 dB, respectively [8]. Each incoming connection request is represented by the tuple $R_i = \{b_i, s_i, d_i, t_i, e_i\}$ where b_i, s_i, d_i, t_i, e_i are the data rate, source node, destination node, arrival time, and holding time of request i, respectively. It is assumed that all of this information is known upon connection arrival.

For each connection request , the Generalized Signal-to-Noise Ratio (GSNR) is computed using (1), with the power of amplified spontaneous emission noise (P_{ASE}) and the power of nonlinear interference (P_{NLI}) for each link individually calculated using (2) and (3), respectively [8]. In here, P is the launch power, p^r is the set of all links that belong to the route of request R_i,[1] and N^l is the number of spans on link l. n_{sp} is the spontaneous emission factor, h is Planck's constant, and f_r and B_r are the center frequency and bandwidth of request R_i. α and L_s^l are the fiber attenuation coefficient and length of the s^{th} span in link l, respectively. ISRS should also be considered in case the total occupied bandwidth is large enough to cause Raman Scattering. In such case, a variable c^l is used to control whether the ISRS should be included in the calculation. The value of c^l is set to 1 if the total occupied bandwidth on the link l is larger than 5 THz, otherwise it is set to 0 and ISRS is not considered. Calculating P_{NLI} requires obtaining the values of P_{SCI} and P_{XCI} using (4) and (5) [8]. Here λ is the fiber nonlinear coefficient. It is necessary to first determine two parameters ϕ_r and $\phi_{r,r'}$ using equation $\phi_r = \beta_2 + 2\pi\beta_3 f_r$ and $\phi_{r,r'} = (\beta_2 + \pi\beta_3(f_r + f_{r'}))(f_{r'} - f_r)$, where β_2 and β_3 are the group velocity dispersion (GVD) parameter and its linear slope, respectively. The SNR_{th} of a MF indicates the lowest allowable SNR for a request; therefore a high value of the request's SNR is desired. The required SNR threshold (SNR_{th}) varies across different MFs, with lower-order MFs requiring lower thresholds. A lower MF requires more FSs to support the same data rate. As the number of FSs used by a request increases, it introduces greater interference to adjacent requests. Although a lower MF has a lower (SNR_{th}) requirement, blindly selecting it to meet the SNR constraint can lead to excessive resource consumption by a single request and increased interference to neighboring requests. Therefore, the selection of the frequency band as well as the selection of the proper MF is crucial in increasing the signal SNR.

For an incoming connection request, SNR_{th} of a candidate MF decides whether the spectrum can be allocated with this MF based on the impairments caused by the occupied adjacent FSs. With an increase in MF level, the SNR_{th} of the request increases and more requests can be blocked due to insufficient SNR, resulting in higher bandwidth blocking probability (BBP). Thus, although a higher MF saves spectrum, it blocks the occupancy of nearby FSs because of the higher SNR_{th}. For the same path, if a lower MF is chosen, more spectrum will be required but the adjacent FSs will be allowed to be occupied due to lower SNR_{th}. The objective of our RMBSA problem is to decrease the BBP by maintaining a proper balance between spectrum utilization and the number of allowable requests. As mentioned in Section I, fragmentation is impacted by two main factors: the spectral gap between two requests, and departure time of requests. Consequently, these factors may also contribute to variations in network capacity. To illustrate these effects, we explore how these parameters affect network performance. To describe spectral gap, we consider the gap between the First Index (FI) of the FSs in a new connection and the Last Index (LI) of the spectrally closest existing request on the lower FS index side, as well as the gap between the LI of the new connection's FSs and the FI of the closest request on the higher FS index side. Based on (1), (3), and (5), when a connection has wider spectral gap from existing ones, it is generally expected to achieve a higher SNR. However, assigning requests with as large a gap as possible with existing requests could exacerbate

[1]We drop the subscript i from variables for simplicity.

fragmentation. Consider the example shown in Fig. 1(a). If new requests are assigned the red FSs, it will cause severe QoT impact on the existing request in blue. On the other hand, assigning the yellow FSs to the new request will not impact the QoT of the existing request substantially, but it will disrupt the 12 consecutive FSs that could have been used by one request.

$$\mathrm{GSNR}^r = \frac{P}{P^r_{\mathrm{ASE}} + P^r_{\mathrm{NLI}}}. \tag{1}$$

$$P^r_{\mathrm{ASE}} = \sum_{l \in p^r} \sum_{s=1}^{N_l} 2 n_{\mathrm{sp}} h f_r B_r \left(e^{\alpha L^l_s} - 1 \right), \tag{2}$$

$$P^r_{\mathrm{NLI}} = \sum_{l \in p^r} \left(P^{r,l}_{\mathrm{SCI}} + P^{r,l}_{\mathrm{XCI}} \right). \tag{3}$$

$$\begin{aligned} P^{r,l}_{\mathrm{SCI}} = N_l \frac{8}{81} \frac{\lambda^2 P^3}{\pi \alpha^2} \frac{1}{\phi_r B_r^2} \\ \left[\frac{(2\alpha - c^l D^l P C_r f_r)^2 - \alpha^2}{\alpha} \mathrm{asinh}\left(\frac{3\pi}{2\alpha} \phi_r B_r^2 \right) \right. \\ \left. + \frac{4\alpha^2 - (2\alpha - c^l D^l P C_r f_r)^2}{2\alpha} \mathrm{asinh}\left(\frac{3\pi}{4\alpha} \phi_r B_r^2 \right) \right], \end{aligned} \tag{4}$$

$$\begin{aligned} P^{r,l}_{\mathrm{XCI}} = N_l \frac{16}{81} \frac{\lambda^2 P^3}{2\pi^2 \alpha^2} \sum_{r'} \frac{1}{\phi_{r,r'} B_{r'}} \\ \left[\frac{(2\alpha - c^l D^l P C_r f_{r'})^2 - \alpha^2}{\alpha} \mathrm{atan}\left(\frac{\pi^2}{\alpha} \phi_{r,r'} B_r \right) \right. \\ \left. + \frac{4\alpha^2 - (2\alpha - c^l D^l P C_r f_{r'})^2}{2\alpha} \mathrm{atan}\left(\frac{\pi^2}{\alpha} \phi_{r,r'} B_r \right) \right]. \end{aligned} \tag{5}$$

In scenarios where higher SNR is preferred, one possible approach is to allocate new connections in frequency gaps that provide greater separation from existing ones. However, this practice can lead to the division of contiguous spectrum resources into disjointed segments, contributing to network fragmentation. Whether this fragmentation results from an effort to maximize SNR or from variations in connection departure times, a notable outcome is the increasing presence of non-contiguous available FS blocks. This is illustrated in Fig. 1(b). Suppose the requests in red blocks are going to leave the network around time point X, and the ones in yellow blocks are going to leave the network around time point Y. If X and Y are not close to each other, after the X time point, in the first scenario there will be three FS blocks that can be used by new requests with sizes of 3, 4, and 8 FSs. But if we put red requests close to each other, as in the second scenario, we can have 2 blocks of FSs free to be used with sizes of 12 and 8 FSs. In this way, requests with larger data rate can be accommodated in the second scenario but not in the first scenario.

Although the total amount of spectral resources remains unchanged, spectrum contiguity may prevent these resources from being fully utilized, leading to a reduction in the effective capacity. Because network traffic is dynamic, with connection arrivals and departures occurring unpredictably, fragmentation may become even more pronounced over time. If departure times are not considered during resource allocation, connections with significantly different lifetimes may be placed adjacent to each other. As these connections terminate and release resources sequentially, they can further contribute to spectral fragmentation. To mitigate this issue, it is important to take both SNR optimization and the departure times of connections into account during resource allocation. Thus, three key parameters - SNR, the FI and LI of FS, and departure time - should be jointly considered in the allocation algorithm to balance spectral efficiency and fragmentation control.

Table I: Number of FSs required for different data rates under each MF (from [1]).

	Modulation Formats				
Bitrate(Gbps)	**BPSK**	**QPSK**	**8 QAM**	**16 QAM**	**32 QAM**
40	6	3	3	3	3
80	9	6	3	3	3
120	12	6	6	3	3
160	15	9	6	6	3
200	18	9	6	6	6

III. The 3MRA Algorithm

We present our 3MRA algorithm in this section. The goal of 3MRA when assigning spectrum to a new request is to let the remaining FSs be available for other requests to the greatest extent possible. To enable it, we rely on the Slice Window (SW) concept first proposed in [2]. An SW is a set of contiguous FSs with the width as the incoming request's requirement, which is calculated using the data rate and the MF of the request. All sets of contiguous and vacant FSs with width of SW with availability along all links of the path are considered as candidate SWs. In this algorithm, the C and L bands are treated equally in terms of assignment. Indeed, the algorithm focuses on resource allocation over all available bands, and therefore can be easily extended to other bands with available PLI models. The selection of SWs is performed based on the availability within the given spectrum constraints, ensuring flexibility in allocation while maintaining the required SNR thresholds. The 3MRA algorithm considers three metrics with different weights including the SNR of each SW, the FI and LI of the FSs of the SW, and the departure time of the request.

In the resource allocation process for each incoming request, 3MRA performs calculations based on (6), with notations given in Table II. Here, $\Phi^{s,m}_{R_i}$ represents the normalized calculated 3-metrics value for the s^{th} candidate SW using MF m for a request R_i.

This value is obtained by summing three components. The first component is the SNR value, normalized across all candidate SWs. The second component is derived from the spectral gap between the FI of FSs in the SW and the LI of FSs in the nearest request on its left, combined with the gap between the LI of FSs in the SW and the FI of FSs in the nearest request on its right. This difference is then normalized across all candidate SWs. The third component corresponds to the departure time, calculated by summing the differences between the departure times of the incoming request and those of the nearest requests on either side of the SW, and normalized across all SWs. By calculating $\Phi^{s,m}_{R_i}$ for each candidate SW, 3MRA bases its resource allocation decisions on these values. It is important to note that the SNR and FS index parameters counterbalance each other. While a higher FS index may contribute to increased fragmentation, it also improves SNR performance. Therefore,

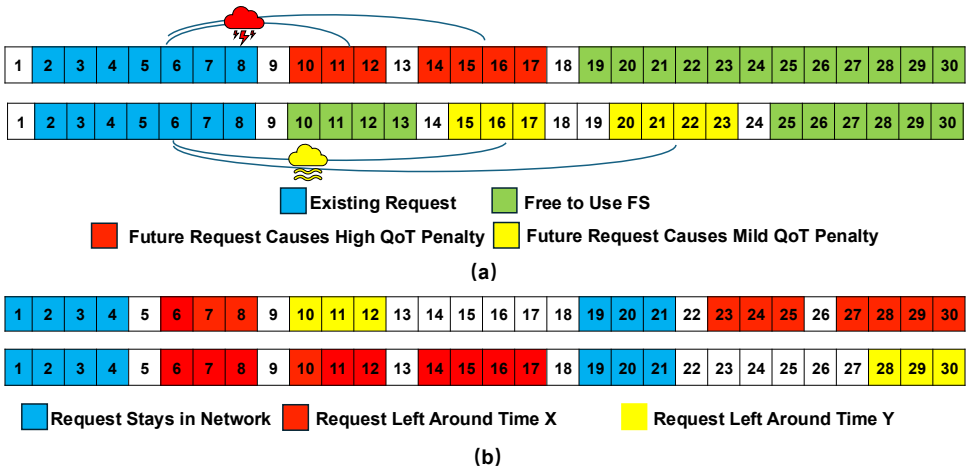

Figure 1: (a): Impact of SNR and FS index. (b) Impact of departure time.

its weight in the calculation remains positive, as our goal is not to minimize it but to balance its impact.

$$\Phi_{R_i}^{s,m} = \gamma \frac{Q_s - Q_l}{Q_h - Q_l} + \eta \frac{(f_s^0 - f_l^{-1}) + (f_r^0 - f_s^{-1}) - 1}{F - (2\xi_i^m + 2)} + \tau \frac{(t_s^D - t_l^D) + (t_s^D - t_r^D)}{T}. \quad (6)$$

Table II: Notation Table

Symbol	Description
$\Phi_{R_i}^{s,m}$	Normalized 3-metrics value for the sth candidate SW of request R_i
R_i	Network request with rate b_i, source node s_i, destination node d_i, arrival time t_i, and duration time e_i
γ	Weight related to the SNR value
η	Weight related to the FS index
τ	Weight related to departure time
Q_s	SNR value of the sth candidate SW
Q_h	Highest SNR over all available SWs
Q_l	Lowest SNR over all candidate SWs
F	Total number of FSs
f_r^0	FI of FS of right closest request of the chosen SW
f_s^0	FI of FS of the chosen SW
f_l^{-1}	LI of FS of left closest request of the sth candidate SW
f_s^{-1}	LI of FS of the sth candidate SW
ξ_i^m	Number of FSs used by request i with MF m
T	Current time
t_s^D	Departure time of the chosen sth candidate SW
t_l^D	Departure time of the left-side closest request of the chosen SW
t_r^D	Departure time of the right-side closest request of the chosen SW

Since SWs are not necessarily adjacent, a link with F FSs can accommodate at most $F - \xi_i^m + 1$ SWs, given that each SW must occupy at least ξ_i^m FSs. As a result, computing $\Phi_{R_i}^{s,m}$ for every SW requires a significant amount of computational time. An even more time-consuming process is evaluating the impact of selecting an SW for the incoming request on existing connections. Since this calculation involves iterating through all connections that share links with the given connection path and SW, the computational complexity increases drastically as the number of accommodated requests grows. Moreover, the SNR values computed for SWs with adjacent indices, as well as their impact on the SNR of existing requests, do not vary significantly. Therefore, in order to keep the execution time of 3MRA small, we use a select window W, which is the number of candidate SWs to be considered by 3MRA; in other words, not all available SWs are considered as candidates, but only a subset of W SWs which are randomly selected from all available SWs across C and L bands.

The detailed algorithm is explained in Algorithm 1. The inputs to the algorithm are the network topology, request R_i, a list of k-shortest paths between s_i and d_i, the set of ξ_i^m for any data rate b_i under each MF m, stored in V_m, the list of SNR_{th} for each MF, stored in SNR_{th}^M, and the values of γ, η, τ, and W. The algorithm returns resource assignment $l_{R_i}^*(k^*, m^*, s^*)$ where k^*, m^*, and s^* are the index of the path, MF, and SW assigned to request R_i. The route path is determined by the pre-calculated k-shortest path list. Lines 2-43 are one full round of resource assignment for one request; starting from the highest MF the algorithm calculates the required number of FSs of the request on line 6, which is also the size of the required SW. On line 7 the algorithm checks if the SWs with same starting FS index on all links of route P_k are unoccupied, the SNR of each available SW is calculated. The SWs with SNR higher than their corresponding MF's SNR_{th} are stored as a pair of SW index and SNR in a list on lines 12-16. Then on lines 20-24, for each SW in that list, the algorithm calculates the QoT of existing connections with shared links with the incoming request. If the candidate SW can lower the SNR of an existing connection below its MF's corresponding SNR_{th}, the candidate SW and corresponding SNR is deleted from the stored (SW, SNR) pairs. After all candidate SWs are evaluated, the algorithm checks for the $\Phi_{R_i}^{s,m}$ value of every available SW remaining in the list and picks the one with the highest $\Phi_{R_i}^{s,m}$ value as the assignment for the incoming request. If after checking all MFs on all k-shortest paths there is no remaining SW, the incoming request is blocked.

Algorithm 1 3MRA Algorithm

Given: Network topology, incoming connection request R_i, 3MRA weights γ, η, and τ
Path $\leftarrow P_k$, $\Phi_{R_i}^{s,m} \leftarrow 0$, $k \leftarrow 1$, $s^* \leftarrow \varnothing$
while $k \leq K$ **do**
  $m = M$
  while $m>0$ **do**
    Get ξ_i^m from V_m
    Determine set of available candidate SWs, SW_{can}, on P_k
    if $SW_{can} = \varnothing$ **then**
      $k \leftarrow k+1$
      break
    else
      $SW_k \leftarrow$ Randomly select W SWs from SW_{can}
      $j = 1$
      while $j \leq |SW_k|$ **do**
        $s = SW_k[j]$
        Calculate SNR_s
        if $SNR_s \geq SNR_{th}^m$ **then**
          Store s and SNR in (SW, SNR) pair
        end if
        $j \leftarrow j+1$
      end while
      for SW in (SW, SNR) pair **do**
        Calculate existing request e's SNR_e $\forall$ existing requests e
        if not all $SNR_e \geq SNR_{th}^e$ **then**
          Delete SW and SNR From (SW, SNR) pair
        end if
      end for
      if (SW, SNR) pair = $\varnothing$ **then**
        $m \leftarrow m-1$
        continue
      end if
      for each SW in (SW, SNR) pair **do**
        Calculate and Store $\Phi_{R_i}^{s,m}$
        for SW with Highest $\Phi_{R_i}^{s,m}$ **do**
          $k^* = k$, $m^* = m$, $s^* = s$
          Output $l_{R_i}^*(k^*, m^*, s^*)$
        end for
      end for
    end if
  end while
  $k \leftarrow k+1$
end while
if $s^* = \varnothing$ **then**
  Request Blocked
end if

IV. Numerical Results

To assess 3MRA, we perform a simulation-based analysis using the topologies shown in Fig. 2 [13] [14], incorporating dynamic connection requests. Yen's algorithm is used to determine the k-shortest paths, and we use $k = 3$ in the simulation. The simulation comprises 100,000 requests, with an initial warm-up phase of 10,000 requests, for which statistics are not recorded, to allow the network to reach steady state. Requests follow a Poisson arrival process and have unit-mean exponential holding times. For the parameters required in the SNR calculations, we utilize n_{sp} = 1.5, α = 0.2dB/km, β_2 = -21.6ps^2/km, β_3 = 0.14ps^3/km, λ = 1.2 $W^{-1}km^{-1}$, C_r = 0.028 $W^{-1}km^{-1}THz^{-1}$, and set the launch power to 0 dBm [8].

For 3MRA, we first analyze the impact of γ, η, and τ on the BBP, shown in Fig. 3. Dots in Fig. 3 shows the BBP of the

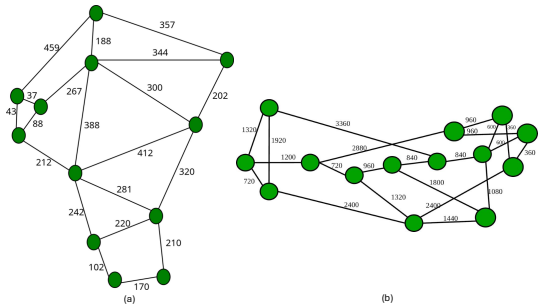

Figure 2: Network topologies: (a) DT (b) NSFNET.

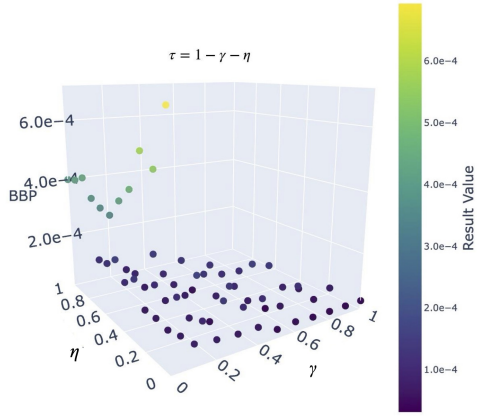

Figure 3: BBP for different weights for DT topology.

combination of different values of γ, η, and τ, with the different colors indicating different values of BBP. To reduce the sample number to an acceptable range, the sum of these three weights is set to 1. Results indicate that the lowest network BBP is achieved when γ is set to 0.6, η to 0.2, τ to 0.2. We use these parameter values for both NSFNET and DT topologies in the rest of the paper.

The selection of W is based on simulation of 3MRA with three different values of W in both the topologies, and the results are shown in Fig. 4 (a) and (b). It can be observed that the curves for $W = 9$ and $W = 12$ almost overlap, while the result for $W = 3$ is noticeably worse than for the other W values. This is because when $W = 9$, the number of available SWs (after feasibility evaluation) is nearly the same as when $W = 12$. However, when $W = 3$, the number of candidate SWs is too limited, making it highly likely that none of the selected SWs can meet the required SNR threshold. As the BBP for $W = 9$ and $W = 12$ are very similar, whereas the BBP for $W = 3$ is significantly higher than that of the other W values, we use $W = 9$ for the rest of the paper. We compare 3MRA with First Fit (FF) with select window of W, and the recently proposed Effect of FM algorithm [15]. The FF algorithm starts from the highest MF and assigns the first (i.e., lowest FS index) SW that meets all requirements. The Effect of FM algorithm prioritizes allocation based on path distance. It searches for available resources in both the C and L bands along the shortest path, giving priority to allocate resources with higher SNR value to the incoming request. The results are shown in Fig. 5 (a) and (b). We observe that 3MRA achieves better BBP in both topologies. Since the average link length in NSFNET topology is longer than that in DT topology, requests

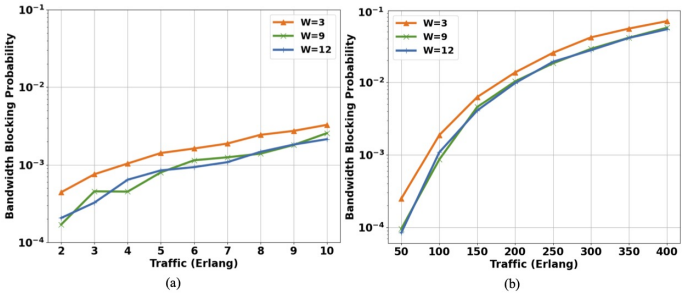

Figure 4: BBP of 3MRA for different values of W for (a) NSFNET (b) DT.

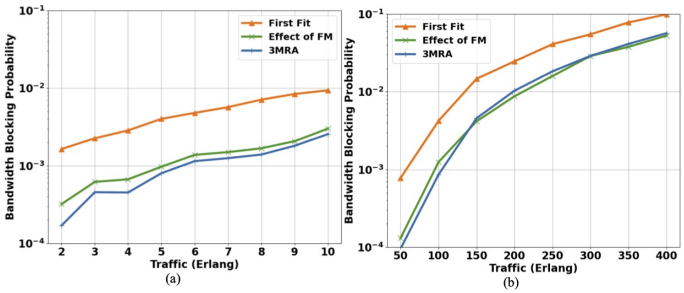

Figure 5: BBP for different loads for (a) NSFNET (b) DT.

in NSFNET topology tend to achieve the lower GSNR values, and more connection requests in NSFNET topology are blocked due to SNR being below the threshold. In DT topology, requests are more likely to be blocked because there is not enough FSs to accommodate the request, that is, due to fragmentation. Since 3MRA can solve the fragmentation problem and leave a larger continuous FS block, although 3MRA achieves higher network capacity in both topologies, the network can have higher arrival rate in DT topology with similar BBP compared to NSFNET topology. Although the performance gap between 3MRA and the FM algorithm is not large in the DT topology, 3MRA offers a significant advantage in computation time (results not shown in paper due to space), making it more suitable for real-time or large-scale scenarios. For example, the running time of 3MRA in the DT topology with 100,000 requests at a load of 300 Erlangs is around 10 minutes, while the FM algorithm takes more than 2 hours. Additionally, we observe a phenomenon from Fig. 6: compared to other algorithms, 3MRA utilizes lower-level modulation formats more frequently. For instance, in the NSFNET topology, 3MRA assigns much more number of requests under the BPSK and QPSK format compared to other algorithms. This indicates that by judiciously utilizing lower-order MFs, 3MRA can reduce the BBP even as network conditions deteriorate (i.e., when the SNR of each request is relatively low). By effectively mitigating network fragmentation, 3MRA preserves a large amount of contiguous spectrum, ensuring that new requests have sufficient contiguous FSs to utilize lower-order MFs. Since lower-order MFs require lower SNR thresholds, this enables the network to accommodate more incoming requests.

V. Conclusion

In this paper, we present an RMBSA algorithm for C+L band in EONs. This method focuses on three parameters: the SNR value of the network request, the FS index of the SW used, and the departure time of the network request. These parameters are used to determine the route, MF, band, and

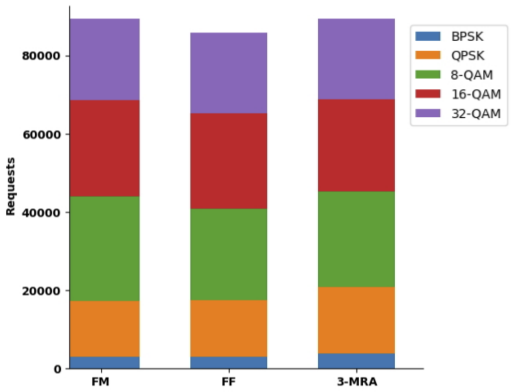

Figure 6: MF distribution in NSFNET with a load of 50 Erlangs.

spectrum information required for allocation and are employed to enhance the SNR of each link, minimize spectrum fragmentation, and ultimately achieve the objective of increasing the overall network capacity. Through simulations, we demonstrated that this method effectively reduces network blocking probability while conserving computation time, compared to other currently proposed methods.

Acknowledgment

This work was supported in part by NSF grant CNS-2210343.

References

[1] C. Rottondi *et al.*, "Crosstalk-Aware Core and Spectrum Assignment in a Multicore Optical Link With Flexible Grid," vol. 67, no. 3, pp. 2144–2156.
[2] S. Petale *et al.*, "TRA: An efficient dynamic resource assignment algorithm for MCF-based SS-FONs," vol. 14, no. 7, p. 511.
[3] J. F. Ramos *et al.*, "Influence of the ROADM architecture on the cost-per-bit in C+L+S multi-band optical networks," in *Proc. of ICTON'23*.
[4] R. S. Luis *et al.*, "Optimizing the Capacity of Standard Cladding Diameter Multicore Fiber Systems Using S, C, and L Bands," in *2023 Conference on Lasers and Electro-Optics Europe & European Quantum Electronics Conference (CLEO/Europe-EQEC)*, pp. 1–1, IEEE.
[5] S. Petale, S.-C. Lin, M. Matsuura, H. Hasegawa, and S. Subramaniam, "PRODIGY: a progressive upgrade approach for elastic optical networks," in *GLOBECOM 2023-2023 IEEE Global Communications Conference*, pp. 2129–2134, IEEE, 2023.
[6] N. Guo *et al.*, "Impact of the band upgrade sequence on the capacity and capital expenditure of multi-band optical networks," vol. 15, no. 10.
[7] P. Poggiolini and M. Ranjbar-Zefreh, "Closed Form Expressions of the Nonlinear Interference for UWB Systems,"
[8] M. Mehrabi *et al.*, "Multi-Band Elastic Optical Networks: Inter-Channel Stimulated Raman Scattering-Aware Routing, Modulation Level and Spectrum Assignment," vol. 39, no. 11, pp. 3360–3370.
[9] B. Correia *et al.*, "QoT Evaluation of Optical Line System Transmission with Bismuth-Doped Fiber Amplifiers in the E-Band," in *Proc. of ACP'21*.
[10] R. K. Jana *et al.*, "Effect of Gain Flattening Filter Placement for Nonlinear-Impairment Mitigation in Multiband Optical Transport Network," in *2023 IEEE International Conference on Advanced Networks and Telecommunications Systems (ANTS)*, pp. 102–107, IEEE.
[11] F. Forghieri, "The GN-model of fiber non-linear propagation and its applications," *Journal of lightwave technology*, vol. 32, no. 4, pp. 694–721, 2013.
[12] Q. Yao *et al.*, "SNR Re-verification-based Routing, Band, Modulation, and Spectrum Assignment in Hybrid C-C+L Optical Networks," pp. 1–1.
[13] I. Sartzetakis *et al.*, "Accurate quality of transmission estimation with machine learning," *Journal of Optical Communications and Networking*, vol. 11, no. 3, pp. 140–150, 2019.
[14] I. Sartzetakis and E. Varvarigos, "Network tomography with partial topology knowledge and dynamic routing," *Journal of Network and Systems Management*, vol. 31, no. 4, p. 73, 2023.
[15] R. K. Jana *et al.*, "Effect of fill margin on network survivability for C+L band optical networks," in *49th European Conference on Optical Communications (ECOC 2023)*, pp. 1453–1456.